

BEAM-SIZE MEASUREMENTS IN THE IPNS 50-MeV TRANSPORT LINE USING STRIPLINE BPMS*

J.C. Dooling[#], F.R. Brumwell, LI. Donley, G.E. McMichael, and V.F. Stipp, Argonne National Laboratory, Argonne, IL 60439, U.S.A.

Abstract

Continuing with the work started two years ago, the technique of using a two-beamlet model to measure beam size is presented[1]. Beam signals are detected on terminated 50-Ω, stripline BPMS located in the transport line between the 50 MeV linac and rapid cycling synchrotron. Each BPM is constructed with four striplines: top, bottom, left and right. Using a fast-sampling oscilloscope to compare the signals from opposite strip lines allows one to determine beam size assuming a two beamlet model. Measurements made with the two-beamlet approach are compared with other standard profile diagnostics such as wire-scanners, segmented Faraday cups, and scintillators. Advantages of the two-beamlet method are that it is non intrusive and does not require the presence of a background gas necessary for an IPM. Disadvantages of the technique are that it does not provide a detailed profile and the longitudinal beam pulse length must be short relative to the stripline length.

INTRODUCTION

A non-intrusive measure of transverse beam size is very desirable, especially in high current, high power machines such as SLC[2], the CERN PS[3] and LHC[4], and the SNS accelerator systems. Such a diagnostic, repeated a number of times along a beamline, could provide real-time transverse emittance measurements. Generally, stripline BPMS have been utilized to provide relatively slow (~kHz) real-time position monitoring and control; however, properly terminated, matched devices can have high bandwidth. Here, we have taken advantage of the bandwidth of our BPMS in the 50 MeV line to examine the temporal behavior of the microbunch structure out of the linac.

ANALYSIS

The longitudinal width measured on the stripline is the sum of both beamlet distributions; however in the calculation, only the adjacent beamlet profile is used. For example, in the present case, beamlet 2 is employed; see Figure 1. Considering the horizontal plane, from geometry, the beam separation half-width, a_x , may be expressed as,

$$a_x = b + x_o - r_{22} \quad (1)$$

where,

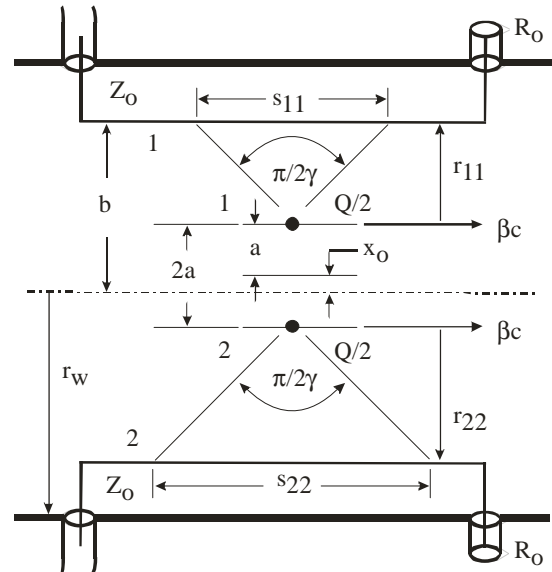


Figure 1: Two-beamlet geometry within a stripline BPM.

$$r_{22} = \frac{s_{22}}{2 \tan\left(\frac{\pi}{4\gamma}\right)} \quad (2)$$

and s_{22} is the charge distribution FWHM length on stripline 2 from beamlet 2. Equation 1 was presented incorrectly in Reference 1 (Eq. 8). Also, x_o is the beam centroid position[5],

$$x_o = \frac{R-L}{R+L} \left(\frac{\phi}{4 \sin(\phi/2)} \right) b \quad (3)$$

where $\phi = 2 \tan^{-1}(w/2b)$ and w is the width of the strip. For our BPM striplines $w=2.9$ cm and $b=3.85$ cm. The length s_{22} is determined by fitting filtered BPM data, corrected for cable attenuation and dispersion, with a double Gaussian waveform along the longitudinal path of the beam. The fitted waveforms are constrained so that the products of amplitude and width for each beamlet are the same (equal charge). In addition, the temporal (longitudinal) centroid positions are also required to be the same. This method can provide reasonable results as long as the temporal bunch profile can be modeled with a single distribution function such as a Gaussian. However, this approach fails when the bunch either bifurcates or its length exceeds that of the stripline.

*Work supported by US DOE, contract no. W-31-109-ENG-38

[#]jcdooling@anl.gov

Data Acquisition

BPM data is acquired using fast, deep-memory digitizing oscilloscopes. Frequency components to the 10th harmonic are necessary for reconstructing the temporal shape of the microbunch; in addition, it is desired to obtain the full linac macropulse injected into the RCS, which for the IPNS linac is typically 70-80 μ s. BPM data is sampled at 5×10^9 samples per second (5 GS/s) for a period of 100 μ s and so a total of 500 kS is collected per channel. The sample rate puts the 10th harmonic (2 GHz) within the Nyquist limit; however, rule-of-thumb sampling (5 times the highest frequency component) would argue for a 10 GS/s rate. Because the present diagnostic is piggy-backed on the existing BPM system, care must be taken to avoid the 205 MHz local oscillator (LO) component. BPM electronics uses the beam centroid position to modulate the 5 MHz difference signal. For the beam size as well as the Energy Spread and Energy Monitor (ESEM)[6] diagnostics, stripline data is analyzed in the frequency domain to correct for cable attenuation and perform Fourier filtering. To avoid interference from the LO, each FFT sample window duration is 400 ns or greater. At 400 ns, the frequency resolution for each window is 2.5 MHz and the 200 MHz component is clearly resolved from the LO. A potentially more serious source of noise is leakage from the 5-MW 200 MHz transmitter driving the DTL tank. Fortunately, the tank is powered before and after the beam pulse, and because these components are deterministic, this noise can be removed via vector subtraction [7]. A cable-corrected spectrum from BPM 1, bottom is presented in Figure 2a). In Figure 2b), the original time data is shown along with the reconstructed waveform determined from Eq. 4. FFT phasing is used for reconstruction of the pulse as is rectangular pulse-train (RPT) phasing. The pulse is reconstructed using the following expression,

$$V(t) = \frac{1}{\sqrt{N_h}} \sum_{n=1}^{N_h} |A_{nN_\lambda}| \cos(2\pi n N_\lambda \Delta f + \theta_{nN_\lambda}) \quad (4)$$

where the summation is made only over the principal harmonics of the microbunch structure, that is the harmonics of the linac frequency. Cable attenuation correction is included in the coefficients, A_{nN_λ} . As mentioned above, for a 400-ns data window, the resolution frequency, $\Delta f=2.5$ MHz, and principal harmonics occur every 80th bin; i.e., $N_\lambda=80$. The phase angle is expressed as,

$$\theta_n = \begin{cases} \tan^{-1} \left(\frac{\text{Im}(S_{f_n})}{\text{Re}(S_{f_n})} \right) + \theta_{d_n}, & \text{FFT} \\ \left(-\frac{n}{N_\lambda} \right) \omega N_\lambda \left(\frac{T_o}{2} + \frac{\tau_b}{2} \right), & \text{RPT} \end{cases} \quad (5)$$

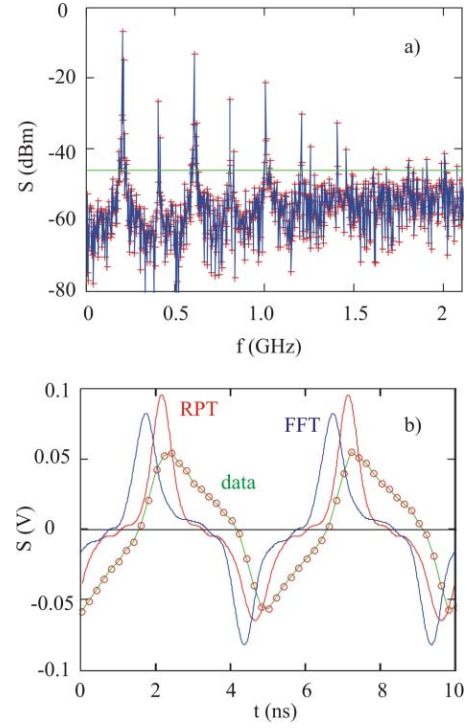


Figure 2: a) Attenuation-corrected BPM 1 spectrum and b) reconstructed time waveforms with FFT and RPT phasing. Original data is also shown.

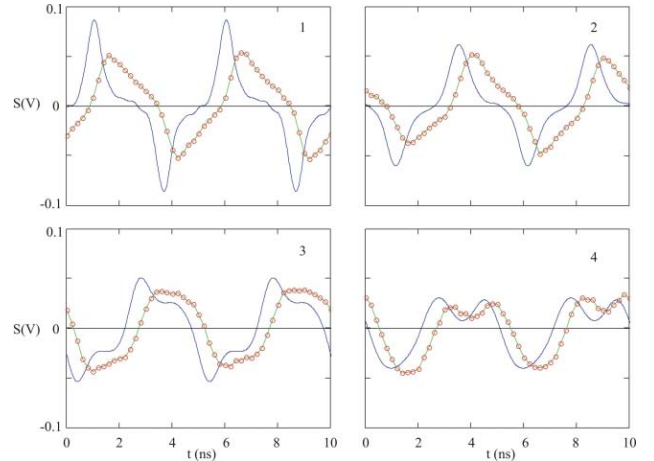


Figure 3: Filtered beam profiles and raw data from the bottom striplines of BPMs 1, 2, and 3, and beam left BPM at position 4.

where S_{f_n} is the complex-valued, Fourier transform of the stripline voltage for frequency bin n , T_o is the period of the linac signal (5 ns) and τ_b is the FWHM pulsewidth of the microbunch. Because of the requirement in our machine to sample for 400 ns, the bunch waveform is an average over 80 linac rf cycles. In addition to amplitude correction, proper account must be made for dispersion in the coaxial transmission lines (RG-213); this affects the phase of the frequency components. The dispersion in radians must be numerically equal to the attenuation in

nepers[8,9,10]. Attenuation scales approximately as \sqrt{f} , though the values used here come from a fit to published data. In Eq. 5, dispersion adjustment is made to the phase with θ_d . The attenuation coefficient in nepers per meter is expressed as,

$$\alpha(\omega) = 3.78 \times 10^{-3} L_c(\omega)$$

where $L_c(\omega)$ is the fit to attenuation data in dB/100 ft (30.48 m). The dispersion angle in radians is then,

$$\theta_{dj}(\omega) = \alpha(\omega) l_{cj}$$

where l_{cj} is the cable length from BPM j to the oscilloscope. For example, in the case of BPM1, $l_{c1}=63.47$ m. At 1 GHz, $L_c=9.33$ dB, and $\theta_{d1}=-2.26$ rad. In the case of RPT phase reconstruction, only the amplitude correction is required. Data from the first four BPMs in the 50 MeV line are presented in Figure 3. The BPMs locations in the line are indicated in Figure 4.

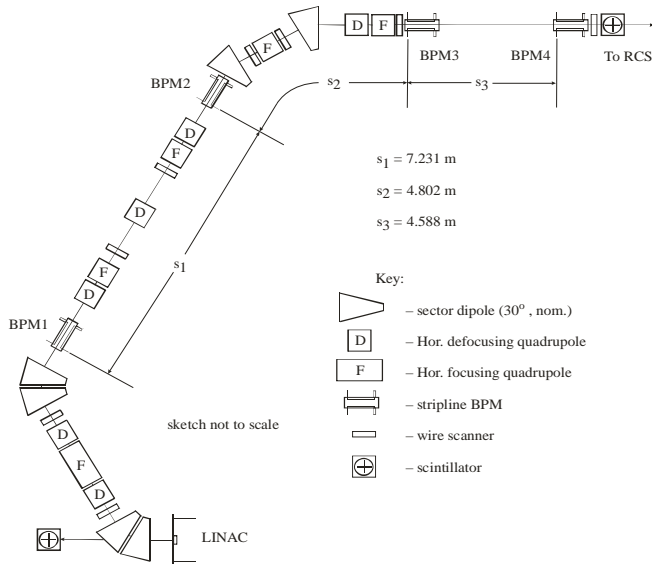


Figure 4: Beam element and diagnostic locations in the upstream portion of the 50 MeV line.

Beam Size Measurements

For the present experiment, the beam size was varied using two upstream quadrupoles as shown in Figure 5. We had hoped to be able to measure the change in horizontal beam size; however, the BPM pulses are bifurcated as shown in Figure 3. Investigating the individual lobes of the temporal distributions, making the assumption they are in fact representative of the beam, yields a non-physical result for beam size ($a_x < 0$); however the trailing lobe does show a size change in the proper direction, $2\Delta a_x = +0.34$ cm. Separately, eight measurements using RPT phasing at BPM1 (upstream of

the quadrupoles used to vary the beam size) indicate a vertical beam height of $2a_y = 1.45$ cm \pm 0.19 cm approximately midway through the linac macropulse; discarding the highest and lowest values in this sample yields $2a_y = 1.48$ cm \pm 0.12 cm. TRACE3D predicts $y_{\max} = 1.0$ cm at the BPM 1 location Wire scanner 3, just downstream of the quadrupole doublet after BPM1 indicates a vertical FWHM value of 0.81 cm. TRACE3D predicts the beam is approximately 10 percent smaller here than at BPM 1. It is not clear why the BPM1 beam size measurement indicates a larger vertical size.

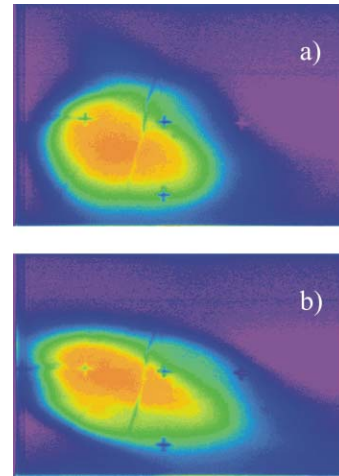


Figure 5: Scintillator near BPM 4; a) nominal quad current and b) current adjusted to broaden the horizontal profile. Fiducial markings indicate a separation of 1 cm.

REFERENCES

- [1] J. C. Dooling, et al., Proc. 22nd LINAC Conf., Lübeck, Germany, Aug. 16-20, 2004, p. 405.
- [2] R. Miller, et al., Proc. 12th Inter. Conf. On High-Energy Accel., Fermilab, Aug. 11-16, 1983, p. 602.
- [3] A. Jansson and D. J. Williams, Nuc. Instrum. Meth. Phys. Res., Sect. A, **479**, 233 (2002).
- [4] A. Jansson, Phys. Rev. STAB, **5**, 072303(2002).
- [5] R. E. Shafer, Proc. 1989 Accel. Instrum. Workshop, BNL, AIP Conf. Proc. **212**, 26(1990), and R. E. Shafer, Proc. 1993 Beam Instrum. Workshop, Santa Fe, AIP Conf. Proc. **319**, 303(1994).
- [6] J. C. Dooling, et al., Proc. 20th LINAC Conf., SLAC-R-561, Monterey, CA, August 2000, p 193.
- [7] J. C. Dooling, Proc. 2004 Beam Instrum. Workshop, Knoxville, AIP Conf. Proc. **732**, 253(2004).
- [8] R. E. Shafer, private communication.
- [9] J. A. Stratton, *Electromagnetic Theory*, McGraw-Hill, New York, 1941, p. 551.
- [10] H. Riege, "High-Frequency and Pulse Response of Coaxial Transmission Cables with Conductor, Dielectric and Semiconductor Losses," CERN Report 70-4, Feb. 1970.